BMC Pulmonary Medicine

RESEARCH

Open Access

Comprehensive analysis pinpoints CCNA2 as a prognostic and immunological biomarker in non-small cell lung cancer

Liming Zhang[1], Shaoqiang Wang[2] and Lina Wang[3*]

Abstract

Background Lung cancer is a leading cause of morbidity and mortality globally. Despite advances in targeted and immunotherapies, overall survival (OS) rates remain suboptimal. Cyclin-A2 (CCNA2), known for its upregulation in various tumors and role in tumorigenesis, has an undefined function in non-small cell lung cancer (NSCLC).

Methods We analyzed three microarray datasets from the Gene Expression Omnibus (GEO) repository to identify differentially expressed genes. Using STRING, we constructed a protein-protein interaction (PPI) network to pinpoint hub genes. The expression and prognostic relevance of CCNA2 were validated using GEPIA and the Kaplan-Meier plotter. Clinicopathological correlations were assessed via the Human Protein Atlas (HPA) and UALCAN databases. qRT-PCR and immunohistochemistry (IHC) were performed to validate CCNA2 mRNA and protein levels. Loss-of-function assays in lung cancer cell lines evaluated the biological role of CCNA2. Immune infiltration and single-cell sequencing were also explored.

Results Analysis of GSE18842, GSE101929, and GSE116959 datasets identified 321 upregulated and 623 downregulated genes in NSCLC. CCNA2 was confirmed to be highly expressed in NSCLC through qRT-PCR and IHC, with overexpression correlating with advanced pathological stages and lymph node metastasis. The area under the curve (AUC) of CCNA2 indicating high diagnostic accuracy. Immune infiltration and single-cell sequencing revealed that CCNA2 expression was significantly associated with immune cell infiltration, particularly in Tprolif cells.

Conclusion CCNA2 is upregulated in NSCLC and shows significant correlation with clinicopathological characteristics. Our findings suggest that CCNA2 may serve as a promising biomarker for both the prognosis and diagnosis of NSCLC.

Keywords Cyclin-A2 (CCNA2), Non-small cell lung cancer (NSCLC), Prognosis, Diagnosis, Immune infiltration, Bioinformatics analysis

*Correspondence:
Lina Wang
wanglina_china@163.com
[1]Department of Thoracic Surgery, Weifang Second People's Hospital, Weifang, Shandong Province 261041, PR China
[2]Department of Thoracic Surgery, Weifang People's Hospital, Weifang, Shandong Province 261000, PR China
[3]Medical Research Center, Affiliated Hospital of Jining Medical University, Jining Medical University, 89 Guhuai Road, Jining, Shandong Province 272029, PR China

Introduction

According to the recent global cancer statistics 2022, lung cancer accounted for nearly 2.5 million of the new cancer cases diagnosed, marking it as the most common type of cancer. Additionally, it was the foremost cause of cancer-related mortality, with approximately 1.8 million deaths, which equates to 18.7% of all cancer fatalities [1]. Lung cancer, categorized into various histopathological types, is predominantly segmented into non-small cell lung carcinoma (NSCLC) and small cell lung carcinoma (SCLC), with NSCLC being the predominant form. Presently, the therapeutic arsenal for lung cancer encompasses surgery, chemotherapy, targeted therapy, and immunotherapy, all of which have collectively contributed to a notable enhancement in patient survival rates [2]. Nonetheless, the majority of patients diagnosed at an advanced stage still face a disappointingly low overall survival (OS) rate. Consequently, there is an imperative need to delve into the etiology and pathogenesis of lung cancer to uncover novel and potential biomarkers that could serve as indicators for prognosis and diagnosis.

Cyclin-A2 (CCNA2), a member of the evolutionarily conserved Cyclin family, is predominantly nuclear-localized and serves as a pivotal regulator of cell cycle progression, playing a crucial role in DNA replication and cell mitosis [3]. CCNA2 has been shown to stimulate the proliferation of specific cell types, including cardiomyocytes and cochlear progenitor cells [4, 5]. Furthermore, it is implicated in the regulation of the epithelial-mesenchymal transition (EMT) through its interaction with the b-catenin and phospholipase C pathways [6]. The long non-coding RNA AFAP1-AS1 has been recognized to suppress cell proliferation in oral squamous cell carcinoma by targeting CCNA2 [7]. In the context of triple-negative breast cancer, CCNA2 is notably overexpressed, and its elevated levels are associated with enhanced cancer cell proliferation, invasion, and metastasis [8]. Nucleolar and spindle-associated protein 1 (NUSAP1), a critical mitotic regulator, is also influenced by CCNA2, where its inhibition can attenuate NUSAP1-induced proliferation and cell cycle progression in osteosarcoma cells [9]. Recent research findings indicate that CCNA2 serves as a molecular target for predicting the prognosis of adenoid cystic carcinoma [10]. In addition, miR-219-5p inhibits cell proliferation and cell cycle progression in esophageal squamous cell carcinoma by targeting CCNA2 [11].

In the present study, the GEO datasets were utilized to screen the differentially expressed genes (DEGs) and the hub genes were identified alongside. While a wealth of evidence implicates CCNA2 in the pathogenesis of diverse cancer types, there exists a notable scarcity of research specifically addressing its role within NSCLC. Thus, we selected CCNA2 after undertaking an exhaustive analysis and leveraging data from multiple databases to delineate CCNA2 expression profiles and to ascertain its prognostic significance in NSCLC. This research aims to delineate the expression patterns of CCNA2 in NSCLC and to evaluate its clinical significance, thereby exploring the potential of CCNA2 as a novel diagnostic and prognostic biomarker for NSCLC.

Materials and methods

Data download

Gene Expression Omnibus (GEO) is a gene expression database created and maintained by the National Center for Biotechnology Information (NCBI). We downloaded 3 datasets from GEO: GSE18842, GSE101929 and GSE116959 (Selection criteria: NSCLC tissue, Sample size > 50) [12]. The 3 datasets consist of 46, 31, 57 tumor samples and 45, 34, 11 adjacent normal lung tissues, respectively. A total of 224 samples including 134 tumor samples and 90 adjacent normal lung tissues were analyzed in this study.

Identification of differentially expressed genes (DEGs)

GEO2R analysis was used in GEO database to divide the samples into normal samples and tumor samples. The gene expression information was obtained, and the genes were screened to get the differentially expressed genes with Adjusted *P*-values (Adj.*p*) < 0.05 and log2-fold-change |FC| > 1 were used as thresholds.

GO and KEGG enrichment analysis

The DAVID website (https://david.ncifcrf.gov/) is a health information database with systematic biological function annotation information for a large number of genes and proteins [13, 14]. The up-regulated and down-regulated DEGs were analyzed by gene ontology (GO) and Kyoto Encyclopedia of Genes and Genomes (KEGG) using the DAVID database to explore the possible biological process (BP), cellular component (CC), molecular function (MF), and pathways involved. The Bioinformatics (http://www.bioinformatics.com.cn/) was used to visualize the enrichment analyses.

Construction of PPI and hub gene screening

The STRING database (https://cn.string-db.org/) is a database for searching known and predicted protein-protein interaction (PPI) [15]. The PPI network of DEGs were constructed and hub genes screened from the STRING (Version 11.5) database, with results visualized by Cytoscape (V 3.9.1) via CytoHubba and MCODE plugins to identify the most important modules in the PPI network [16].

Hub gene expression and survival analysis

Gene Expression Profiling Interactive Analysis (GEPIA) (http://gepia.cancer-pku.cn/) is a public database with RNA-seq expression data of 9736 tumor samples and 8587 normal samples from TCGA and GTEx projects [17]. GEPIA database was used to analyze the expression of the above genes in lung adenocarcinoma (LUAD) and lung squamous cell carcinoma (LUSC).

The Kaplan-Meier plotter (http://kmplot.com/analysis/) integrates microarray data from GEO and TCGA to provide prognostic information for various cancers including lung cancer [18]. We used this database to perform survival analysis of the selected hub genes.

Expression of CCNA2 in pan-cancer and NSCLC

We downloaded the RNAseq data in FPKM format from the ALL (pan-cancer), LUAD and LUSC project in TCGA (https://portal.gdc.cancer.gov/) and used log2-transform the data. The R package ggplot2 was applied to analyze and visualize the expression of CCNA2 in different cancer types.

CCNA2 expression in lung cancer of human protein atlas

The human protein atlas (HPA) (www.proteinatlas.org) is an open database, with transcriptomic and proteomic techniques to study protein expression from mRNA and protein levels in different human tissues and organs [19]. By searching the HPA database, the expression of CCNA2 and its antibody CAB000114 in lung cancer and normal tissues were analyzed.

Association of CCNA2 expression with clinicopathological features

The University of ALabama at Birmingham CANcer data analysis Portal (UALCAN) database (https://ualcan.path.uab.edu/index.html) is a comprehensive, user-friendly, and interactive web resource for analyzing cancer OMICS data, enabling users to identify biomarkers and assess gene expression with various clinicopathological features [20, 21]. Utilizing UALCAN website, we aimed to assess the correlation between CCNA2 expression and its relationship with staging, lymph node metastasis, and TP53 mutation in patients with NSCLC.

ROC curve and prognosis analysis

To draw the receiver operating characteristic (ROC) curve, we used the R package pROC to analyze the RNA-seq data in FPKM format from the LUAD and LUSC projects in TCGA database. The ggplot2 package was used for visualization. Then Kaplan-Meier plotter was used to perform survival analyses of CCNA2 in LUAD and LUSC patients, respectively. Univariate and multivariate Cox regression analyses were conducted to identify independent prognostic risk factors, followed by the construction of a nomogram and the development of a calibration curve.

Human lung cancer specimen collection

We collected lung cancer and corresponding para-cancerous tissue samples from 27 lung cancer patients who underwent surgery at our institution. None of the patients had received preoperative treatment. Informed consent was obtained from all participants prior to the study. The Ethics Committee of the Affiliated Hospital of Jining Medical University evaluated and approved this work (Approval number 2021-11-C009).

RNA extraction and qRT-PCR analysis

Samples from 27 cases of lung cancer and para-cancerous tissues were obtained from our hospital. TRIzol reagent was used to extract total cellular RNA (Invitrogen, USA). A commercial cDNA synthesis Kit (SuperScript First-Strand Synthesis System, Thermo Fisher Scientific) was utilized to generate cDNAs through reverse transcription. The SYBR Green Assay Kit was used to detect the presence of mRNA (TAKARA, Japan). Using the Biosystems ViiA7 Sequence Detection System, the qRT-PCR procedure was carried out at least 3 times. Relevant primer synthesis are as follows:

CCNA2 forward primer: 5'-CGCTGGCGGTACTGAAGTC-3',
CCNA2 reverse primer:5'-GAGGAACGGTGACATGCTCAT-3';
GAPDH forward primer:5'-CCAGCAAGAGCACAAGAGGAA-3'.
GAPDH reverse primer:5'-ATGGTACATGACAAGGTGCGG-3'.

Cell culture and siRNA transfection

The human lung cancer cell line A549 [A-549] (CL-0016) was kindly provided by Wuhan Pricella Biotechnology Co., Ltd, authenticated using short tandem repeat (STR) profiling and free of mycoplasma contamination as confirmed by PCR. The cells were cultured in a 37°C CO_2 incubator with RPMI-1640 medium supplemented with 10% fetal bovine serum. The cells were seeded in a six-well plate, and siRNA complexed with Lipofectamine 3000 was added for transfection. The CCNA2 siRNA sequences are as follows:

Hsa-CCNA2-Si-1: sense: 5'-CCTCTTGATTATCCAATGGAT-3';
antisense: 5'- ATCCATTGGATAATCAAGAGG-3'.
Hsa-CCNA2-Si-2: sense: 5'-TCCTAAGCAACTGGATCAATT-3';
antisense: 5'-AATTGATCCAGTTGCTTAGGA-3'.

Cell proliferation assay by cell counting kit-8 (CCK-8)

1×10^3 cells were seeded into a 96-well plate, and 10 μL of CCK-8 solution was added at 0, 24, 48, and 72 h, followed by a 2-hour incubation at 37 °C. The absorbance at 450 nm was analyzed with standard microplate readers (BioTek, Winsky, Vermont, USA).

Scratch wound healing assay

5×10^5 cells were seeded into a six-well plate. The cells were then scratched using a 10 μL pipette tip, followed by washing with PBS. Subsequently, serum-free RPMI-1640 medium was added to continue the culture. Images were captured under a microscope at 0 and 24 h, with analysis performed using ImageJ software.

Transwell assay

Seed 3×10^5 cells and culture them in a six-well plate. Add 600 μL medium to the lower chamber and 100 μL serum-free RPMI 1640 medium to the upper chamber. Incubate at 37 °C for 24, 36, and 48 h. Invert the chamber on absorbent paper to remove the medium, followed by rinsing with PBS. Fix the chamber with 4% paraformaldehyde for 20 min and stain with crystal violet (0.1%) for 15 min. Use a cotton swab to remove non-migrated cells from the chamber. Finally, images were captured under a microscope, and processed by ImageJ software.

Detection of apoptosis by flow cytometry

3×10^5 cells were cultured in a six-well plate. The CCNA2 siRNAs were utilized for cell transfection. Annexin V^+ apoptotic cells were detected 48 h afterwards with flow cytometry.

Relationship between CCNA2 expression and immune infiltration in NSCLC

The MCP-counter and ssGSEA algorithm in the R package GSVA were used to analyze the infiltration enrichment of 24 immune cells, including aDC (activated DC); B cells; CD8 T cells; Cytotoxic cells; DC; Eosinophils; iDC (immature DC); Macrophages; Mast cells; Neutrophils; NK CD56 bright cells; NK CD56 dim cells; NK cells; pDC (plasmacytoid DC); T cells; T helper cells; Tcm (T central memory); Tem (T effector memory); Tfh (T follicular helper); Tgd (T gamma delta); Th1 cells; Th17 cells; Th2 cells and Treg. The association between CCNA2 expression and immune cell infiltration was assessed by Spearman analysis.

The single cell sequencing analysis of CCNA2 in NSCLC

CancerSEA (http://biocc.hrbmu.edu.cn/CancerSEA/) was utilized to investigate the association between CCNA2 and 14 distinct functional states within a comprehensive dataset of 41,900 single cancer cells, representing 25 different types of cancer [22].

Tumor Immune Single-cell Hub 2 (TISCH2) (http://tisch.comp-genomics.org) is a scRNA-seq database focusing on tumor microenvironment (TME) [23]. TISCH2 offers comprehensive, single-cell level annotations, facilitating the in-depth exploration of the TME across a spectrum of cancer types. It encompasses an extensive dataset of 6,297,320 cells derived from 190 distinct studies. Utilizing TISCH2, a detailed single-cell resolution analysis of CCNA2 in NSCLC was conducted.

Statistical analysis

All the statistical data were analyzed by SPSS (Version 22.0) software. The data are expressed as mean ± standard deviation (SD). Subgroup differences between paired tissues were compared using a two-tailed paired t-test. One-way ANOVA was utilized to compare the means across three groups of cell experiment data. $^*P < 0.05$ is considered to be statistically significant.

Results

Identification and analysis of hub genes from the DEGs across 3 GEO datasets

A total of 4508 DEGs in GSE18842, GSE101929 and GSE116959 were obtained after screening (Fig. 1A-C). 321 up-regulated DEGs and 623 down-regulated ones were identified following the intersection of 3 GEO datasets (Fig. 1D-E). GO analysis showed that these DEGs were mainly located in the spindle, mitotic spindle, sarcolemma, with biological functions in nuclear division, mitotic nuclear division, and chromosome segregation (Supplementary Fig. S1A-B). The molecular functions involved actin binding, glycosaminoglycan binding, and sulfur compound binding (Supplementary Fig. S1C). KEGG enrichment analysis showed cell cycle, oocyte meiosis, p53 signaling pathway, Tyrosine metabolism and phenylalanine metabolism (Supplementary Fig. S1D). The PPI network was constructed and the top 10 hub genes were identified that represent the most significant modules within the network: TTK, BUB1B, CCNA2, UBE2C, AURKB, MELK, CCNB2, KIF2C, CDCA8, and NUSAP1 (Fig. 1F).

The mRNA expression of the 10 hub genes in LUAD and LUSC

GEPIA database was explored to validate the differential expression levels of the 10 hub genes between lung cancer tissues and their normal counterparts. Compared to the normal tissues, all the 10 hub genes were expressed significantly high in LUAD and LUSC (Supplementary Fig. 2).

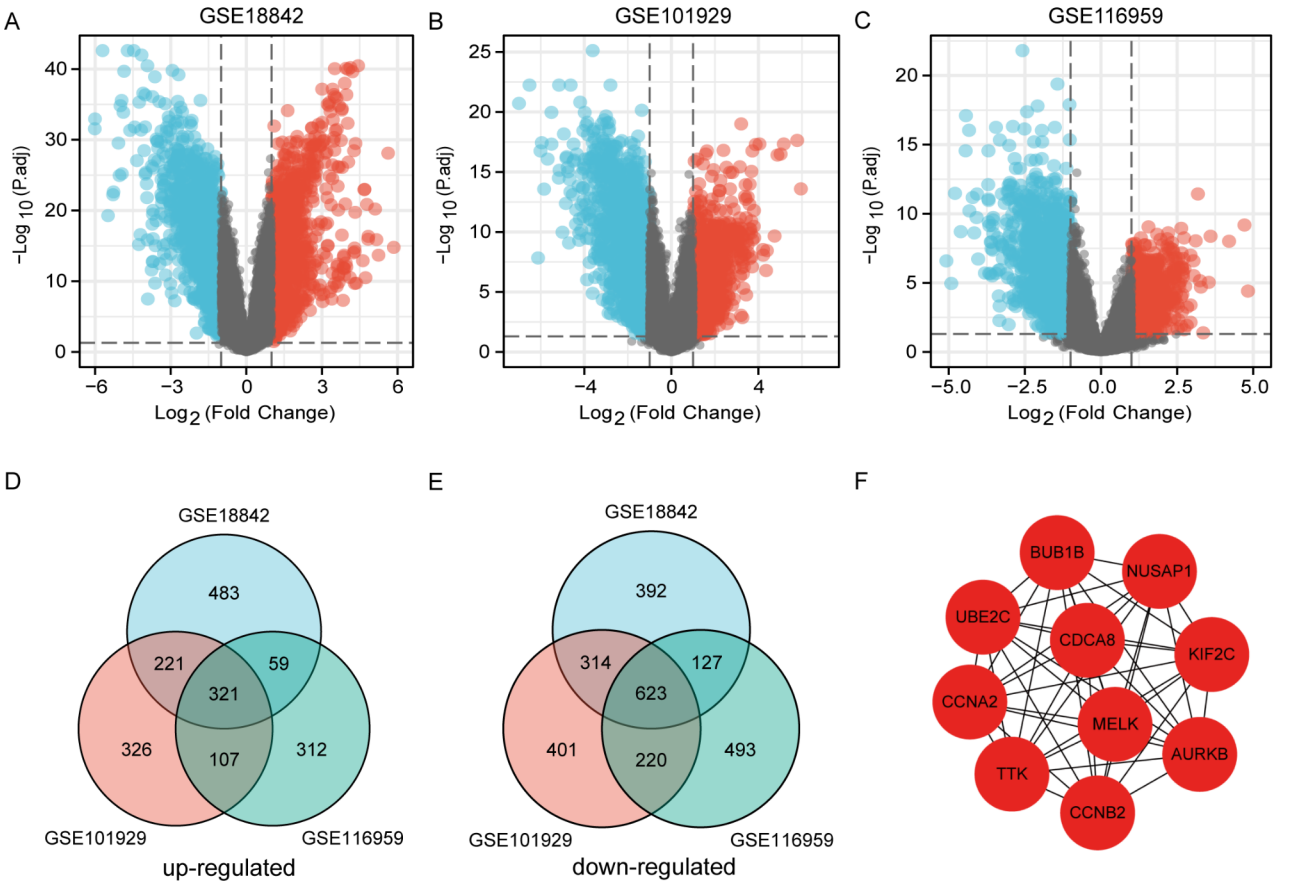

Fig. 1 Identification and analysis of hub genes from the DEGs across 3 GEO datasets. The volcano diagrams illustrating all up-regulated and down-regulated DEGs of GSE18842 (**A**), GSE101929 (**B**), and GSE116959 (**C**). Red represented upregulated genes, blue represented downregulated genes, and grey represented no change. Venn diagram comparing all up-regulated (**D**) and down-regulated (**E**) DEGs of 3 GEO datasets. (**F**) The ten hub genes were identified from PPI network

The prognostic significance of the 10 hub genes in lung cancer patients

Kaplan-Meier plotter was used to evaluate the prognostic value of the above 10 hub genes. The survival curves showed that the 10 hub genes including TTK ($P = 1.0e-16$, HR = 1.77), BUB1B ($P = 2.1e-16$, HR = 1.7), CCNA2 ($P = 1.0e-16$, HR = 1.76), UBE2C ($P = 1.0e-16$, HR = 1.76), AURKB ($P = 1.0e-16$, HR = 1.84), MELK ($P = 4.4e-13$, HR = 1.6), CCNB2 ($P = 4.4e-13$, HR = 1.99), KIF2C ($P = 1.0e-16$, HR = 1.78), CDCA8 ($P = 9.0e-16$, HR = 1.68), and NUSAP1 ($P = 2.0e-16$, HR = 1.7) were all significantly negatively correlated with the prognosis of lung cancer patients (Supplementary Fig. 3). The median survival time for the group with lower expression levels was markedly extended compared to the group with higher expression levels. Thus, an elevated expression of these hub genes was associated with a worse prognosis.

The expression of CCNA2 in pan-cancer and NSCLC tissues

To explore the relationship between CCNA2 and cancers, we first analyzed the expression of paired tumor and non-tumor tissues in pan-cancer of TCGA. Compared to normal tissues, CCNA2 was significantly highly expressed in bladder urothelial carcinoma (BLCA), breast invasive carcinoma (BRCA), cholangiocarcinoma (CHOL), colon adenocarcinoma (COAD), esophageal carcinoma (ESCA), head and neck squamous cell carcinoma (HNSC), kidney chromophobe (KICH), kidney renal clear cell carcinoma (KIRC), kidney renal papillary cell carcinoma (KIRP), liver hepatocellular carcinoma (LIHC), prostate adenocarcinoma (PRAD), stomach adenocarcinoma (STAD), and uterine corpus endometrial carcinoma (UCEC) (Fig. 2A). Of note, CCNA2 mRNA was substantially expressed in LUAD and LUSC tissues (Fig. 2B-C). Consistently, the protein level of CCNA2 was at moderate to high levels in 5 NSCLC tissues, including 1 LUAD with strong staining (Fig. 2D), 1 LUAD with moderate staining (Fig. 2E), 1 LUSC with strong staining

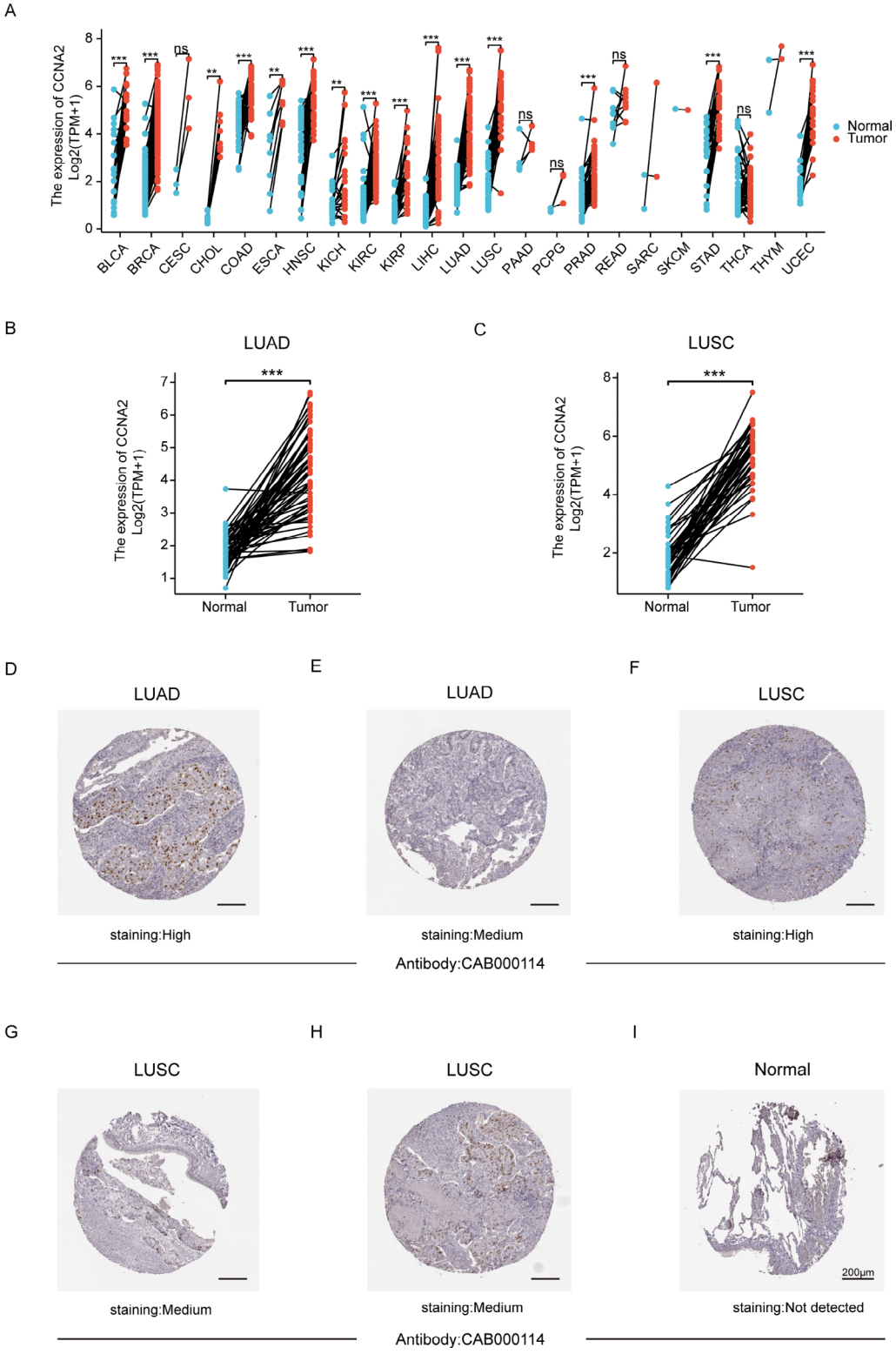

Fig. 2 The expression of CCNA2 in pan-cancer and NSCLC tissues. (**A**) The mRNA expression of CCNA2 in paired pan-cancer tissues in TCGA. The mRNA expression of CCNA2 in paired LUAD (**B**) and LUSC (**C**) tissues and normal tissues of TCGA. (**D**)-(**I**): The protein level of CCNA2 in NSCLC from HPA database. (**D**) 73 years old, male, LUAD, strong staining. (**E**) 57 years old, female, LUAD, moderate staining. (**F**) 82 years old, male, LUSC, strong staining. (**G**) 69 years old, male, LUSC, medium staining. (**H**) 64 years old, male, LUSC, medium staining. (**I**) 43 years old, female, normal. ns, not significant; * $P < 0.05$; ** $P < 0.01$; *** $P < 0.001$

and 2 with moderate staining (Fig. 2F-H), while no obvious staining in normal lung tissue (Fig. 2I) based on HPA. Hence, the obviously elevated mRNA and protein expression of CCNA2 was found in NSCLC.

CCNA2 correlated with clinicopathological features in NSCLC

UALCAN was utilized to explore the relationship between CCNA2 and different clinicopathological characteristics in NSCLC patients, which were further divided into LUAD and LUSC patients. No matter whether in LUAD and LUSC, the CCNA2 expression level was substantially linked with advanced clinical stage, lymph node metastasis and TP53-mutant (Fig. 3A-F). Thus, it is anticipated that CCNA2 might be involved in the progression and metastasis of NSCLC.

The diagnostic and prognostic values of CCNA2 in NSCLC patients

Receiver Operating Characteristic (ROC) curves were generated to assess the diagnostic efficacy of CCNA2 in NSCLC. And the area under the curve (AUC) of CCNA2 in LUAD and LUSC was 0.970 (95% CI: 0.954–0.986) and 0.996 (95% CI: 0.993-1.000), respectively, which demonstrated considerably high accuracy of CCNA2 in NSCLC (Fig. 4A-B).

Kaplan-Meier plotter analysis was carried out to explore the value of CCNA2 in the prognosis of NSCLC. In patients with LUAD, the expression levels of CCNA2 were significantly inversely correlated with patient prognosis. Specifically, the median survival time for patients in the low-expression group of CCNA2 was substantially longer compared to those in the high-expression group (Fig. 4C). Conversely, in LUSC patients, elevated levels of CCNA2 were associated with a prolonged survival time (Fig. 4D). In LUAD, the univariant Cox regression analysis showed that CCNA2 expression, smoking and TNM stage were significantly correlated with OS. The multivariate Cox analysis confirmed that CCNA2 expression and TNM stage were independent indicators of unfavorable OS (Fig. 4E). Afterwards, a nomogram was created to predict the 1-year, 3-year, and 5-year survival of LUAD patients, with the calibration curve to validate the accuracy of the nomogram (Fig. 4F-G). Calibration curves compare the predicted survival probabilities with the actual observed survival rates at specific time points, such as 3 and 5 years. The closer the calibration curve aligns with the ideal line (where the predicted probabilities equal the actual probabilities), the better the model's predictive accuracy. In LUSC, the univariant and multivariate Cox regression analysis indicated Pathological T/M stage and age were independent prognostic risk factor (Supplementary Table 1). Thus, CCNA2 could be served as an independent prognostic risk factor in LUAD.

The oncogenic function of CCNA2 in LUAD cells

To validate the expression of CCNA2 in lung cancer cells, qRT-PCR was conducted in 27 cases of paired lung cancer and para-cancerous tissues. The results showed that CCNA2 was significantly highly expressed in NSCLC tissues (Fig. 5A). Afterwards, cell function assays were performed to explore the fundamental biological roles of CCNA2 in lung cancer cells. SiRNA was transfected in A549 cells to knockdown the expression of CCNA2, and qRT-PCR was employed to confirm the knockdown efficiency (Fig. 5B). Cell proliferation assay by CCK-8 indicated that CCNA2 knockdown could inhibit A549 cell proliferation (Fig. 5C). The scratch wound healing experiment demonstrated that cell migration ability was decreased upon CCNA2 silencing in A549 cells (Fig. 5D). Transwell assay revealed that knockdown of CCNA2 expression could suppress the invasive capability of A549 cells (Fig. 5E). In addition, the flow cytometry analysis showed obviously increased Annexin V^+ cells after CCNA2 silencing in A549 cells (Fig. 5F). Thus, knockdown of CCNA2 expression could impair cell proliferation, migration, and invasion, but increase apoptosis in lung cancer cells.

The relationship between CCNA2 expression and immune infiltration in NSCLC

MCP-counter was used to explore the immune cell infiltration of NSCLC. Based on CCNA2 mRNA median expression, TCGA samples were split into two groups with high and low CCNA2 expression. MCP-counter findings revealed that neutrophil, endothelial cell, T cell $CD8^+$, NK cell, B cell, myeloid dendritic cell, monocyte and macrophage/monocyte are the substantially distinct immune cell types invaded between CCNA2 high and low expression groups in LUAD (Fig. 6A). Additionally, endothelial cell, myeloid dendritic cell, T cell, and B cell are the obviously different immune cells infiltrated between CCNA2 high and low expression groups in LUSC (Fig. 6B).

The ssGSEA algorithm and Spearman analysis was performed to study the association between CCNA2 and 24 types of immune cell infiltration. The results showed that Th2 cells, T gamma delta, and NK CD56 dim cells were all positively correlated with the expression of CCNA2, whereas mast cells, Th17 cells, eosinophils, TFH and iDC were negatively correlated in LUAD (Fig. 6C). In LUSC, Th2 cells, T gamma delta, T helper cells were all positively associated with CCNA2 expression, while pDC, DC, mast cells and NK CD56 bright cells were negatively correlated with CCNA2 expression (Fig. 6D).

The correlation of CCNA2 and the major eight immune checkpoint genes (ICGs) were also investigated. In LUAD, the expression of CCNA2 showed significantly positive relation to CD274 ($R = 0.291$, $P < 0.001$), HAVCR2

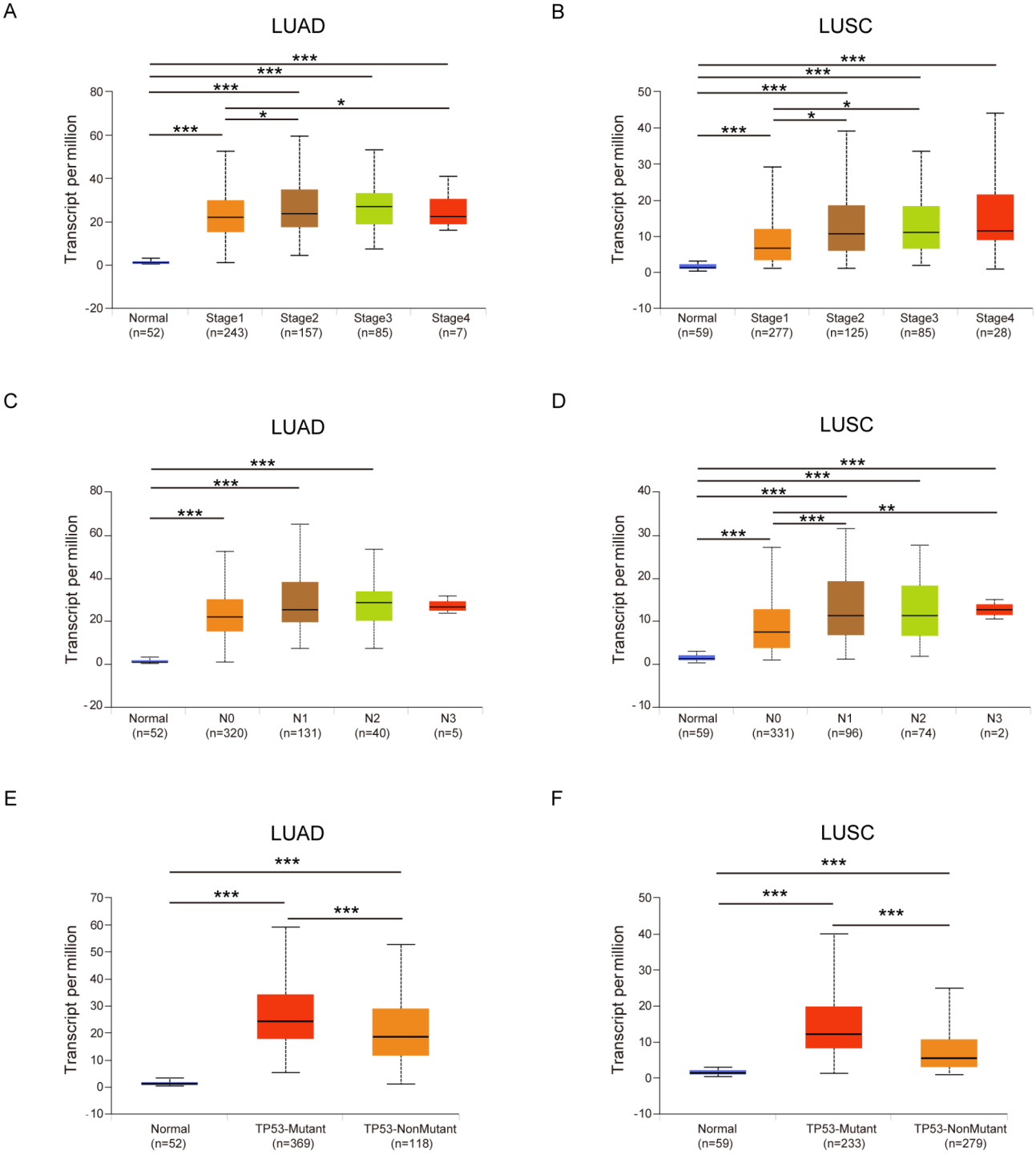

Fig. 3 CCNA2 correlated with clinicopathological features in NSCLC. Relationship between CCNA2 expression and clinical stage of LUAD (**A**) and LUSC (**B**). Relationship between CCNA2 expression and lymph node metastasis of LUAD (**C**) and LUSC (**D**). Relationship between expression of CCNA2 and TP53 mutant of LUAD (**E**) and LUSC (**F**). * $P<0.05$; ** $P<0.01$; *** $P<0.001$

($R=0.188$, $P<0.001$), LAG3 ($R=0.240$, $P<0.001$), PDCD1 ($R=0.176$, $P<0.001$), PDCD1LG2 ($R=0.290$, $P=0.007$) and SIGLEC15 ($R=0.178$, $P<0.001$) (Fig. 6E). In LUSC, the expression of CCNA2 indicated positive relation to CD274 ($R=0.155$, $P<0.001$) and PDCD1LG2 ($R=0.120$, $P=0.007$) (Fig. 6F). Thus, in the tumor environment of NSCLC, CCNA2 is postulated to exert significant influence on the behavior and function of immune cells, which needs further investigation.

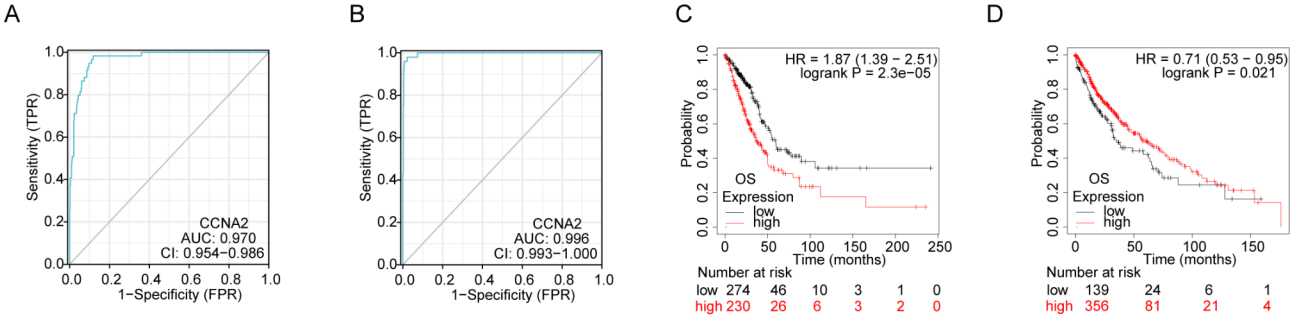

E

Characteristics	Total(N)	Univariate analysis HR (95% CI)	Univariate analysis P value	Multivariate analysis HR (95% CI)	Multivariate analysis P value
Pathologic T stage	527		< 0.001		
T1	176	Reference		Reference	
T2	285	1.507 (1.059 − 2.146)	0.023	1.443 (0.915 − 2.276)	0.115
T3	47	2.964 (1.762 − 4.986)	< 0.001	3.522 (1.867 − 6.644)	< 0.001
T4	19	3.357 (1.767 − 6.376)	< 0.001	2.263 (1.074 − 4.768)	0.032
Pathologic N stage	514		< 0.001		
N0	345	Reference		Reference	
N1	96	2.293 (1.632 − 3.221)	< 0.001	1.971 (1.332 − 2.916)	< 0.001
N2	71	3.133 (2.154 − 4.559)	< 0.001	2.698 (1.749 − 4.163)	< 0.001
N3	2	0.000 (0.000 − Inf)	0.994	0.000 (0.000 − Inf)	0.993
Pathologic M stage	381		0.01		
M0	356	Reference		Reference	
M1	25	2.176 (1.272 − 3.722)	0.005	1.688 (0.917 − 3.108)	0.093
Gender	530		0.57		
Female	283	Reference			
Male	247	1.087 (0.816 − 1.448)	0.569		
Age	520		0.185		
<= 65	257	Reference			
> 65	263	1.216 (0.910 − 1.625)	0.186		
Smoker	516		0.777		
No	74	Reference			
Yes	442	0.942 (0.625 − 1.420)	0.775		
CCNA2	530		< 0.001		
Low	267	Reference		Reference	
High	263	1.709 (1.276 − 2.290)	< 0.001	1.455 (1.030 − 2.055)	0.033

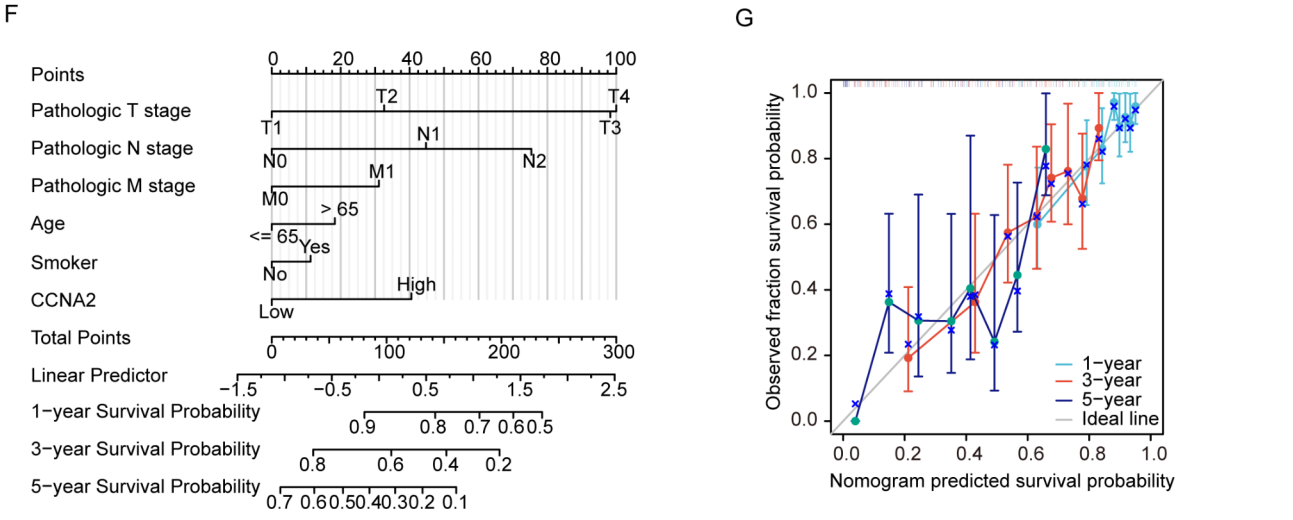

Fig. 4 The diagnostic and prognostic value of CCNA2 in NSCLC patients. The ROC curves of CCNA2 for the diagnosis of LUAD (**A**) and LUSC (**B**). The OS curves of CCNA2 in prognosis of LUAD (**C**) and LUSC (**D**). (**E**) The univariate and multivariate Cox regression analysis of CCNA2 in LUAD. (**F**) Nomogram of CCNA2, smoker, TNM, and age in LUAD to predict the 1-year, 3-year, and 5-year survival. (**G**) Calibration curve to validate the accuracy of the nomogram

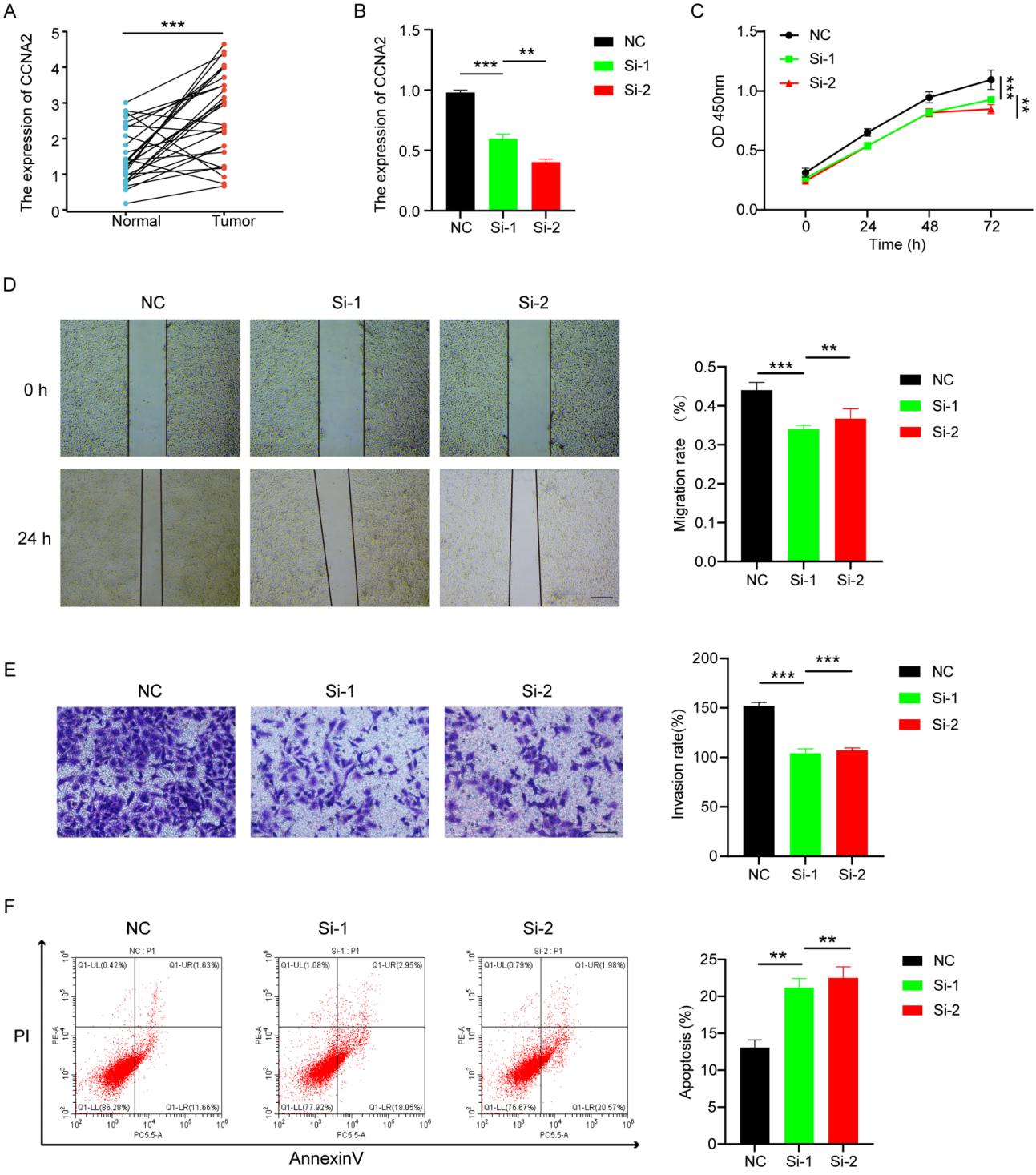

Fig. 5 The oncogenic function of CCNA2 in LUAD cells. (**A**) 27 paired NSCLC and normal tissue was detected by qRT-PCR. (**B**) CCNA2 was knocked down in A549 cells via siRNA transfection. (**C**) CCNA2 knockdown inhibited A549 cell proliferation by CCK-8 assay. (**D**) CCNA2 silencing decreased A549 cell migration ability. (**E**) CCNA2 knockdown impaired A549 cell invasion. (**F**) CCNA2 silencing increased A549 cell apoptosis demonstrated by flow cytometry analysis. * $P<0.05$; ** $P<0.01$; *** $P<0.001$

CCNA2 expression at single-cell level in NSCLC

Single-cell sequencing is a technology for sequencing and studying the genome, transcriptome, and epigenome at the single cell level. We compared and analyzed the single-cell sequencing of CCNA2 in NSCLC by CancerSEA (Fig. 7A). In LUAD, CCNA2 expression was positively correlated with proliferation, cell cycle, DNA damage, invasion, EMT, DNA repair and metastasis

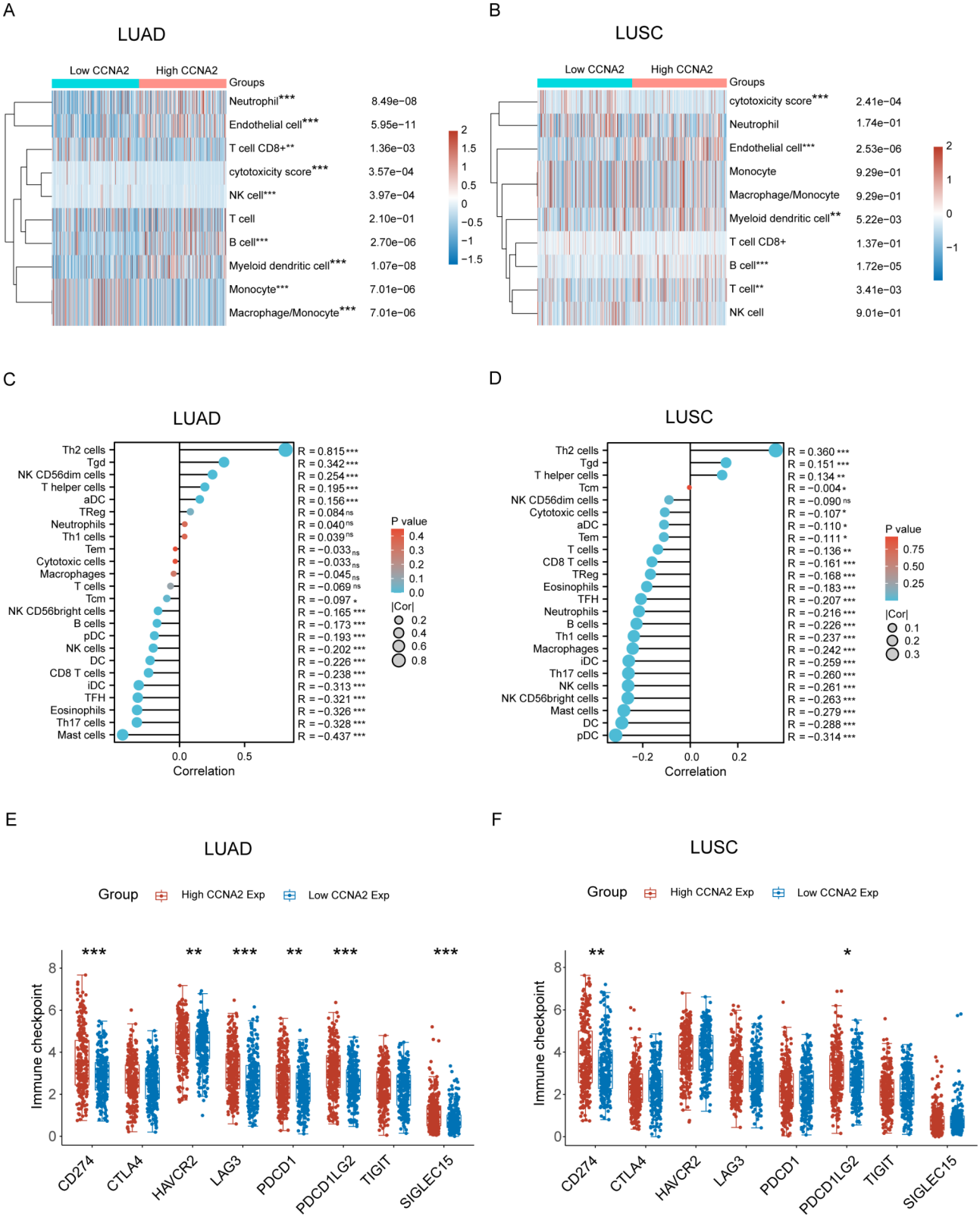

Fig. 6 The relationship between CCNA2 expression and immune infiltration in NSCLC. MCP-counter revealing the association between CCNA2 expression and immune cells infiltration in LUAD (**A**) and LUSC (**B**). Lollipop diagram displaying the correlation between CCNA2 expression and 24 immune cells infiltration in LUAD (**C**) and LUSC (**D**). Box plot comparing the eight ICGs expression between $CCNA2^{high}$ and $CCNA2^{low}$ groups in LUAD (**E**) and LUSC (**F**). ns, not significant; * $P < 0.05$; ** $P < 0.01$; *** $P < 0.001$

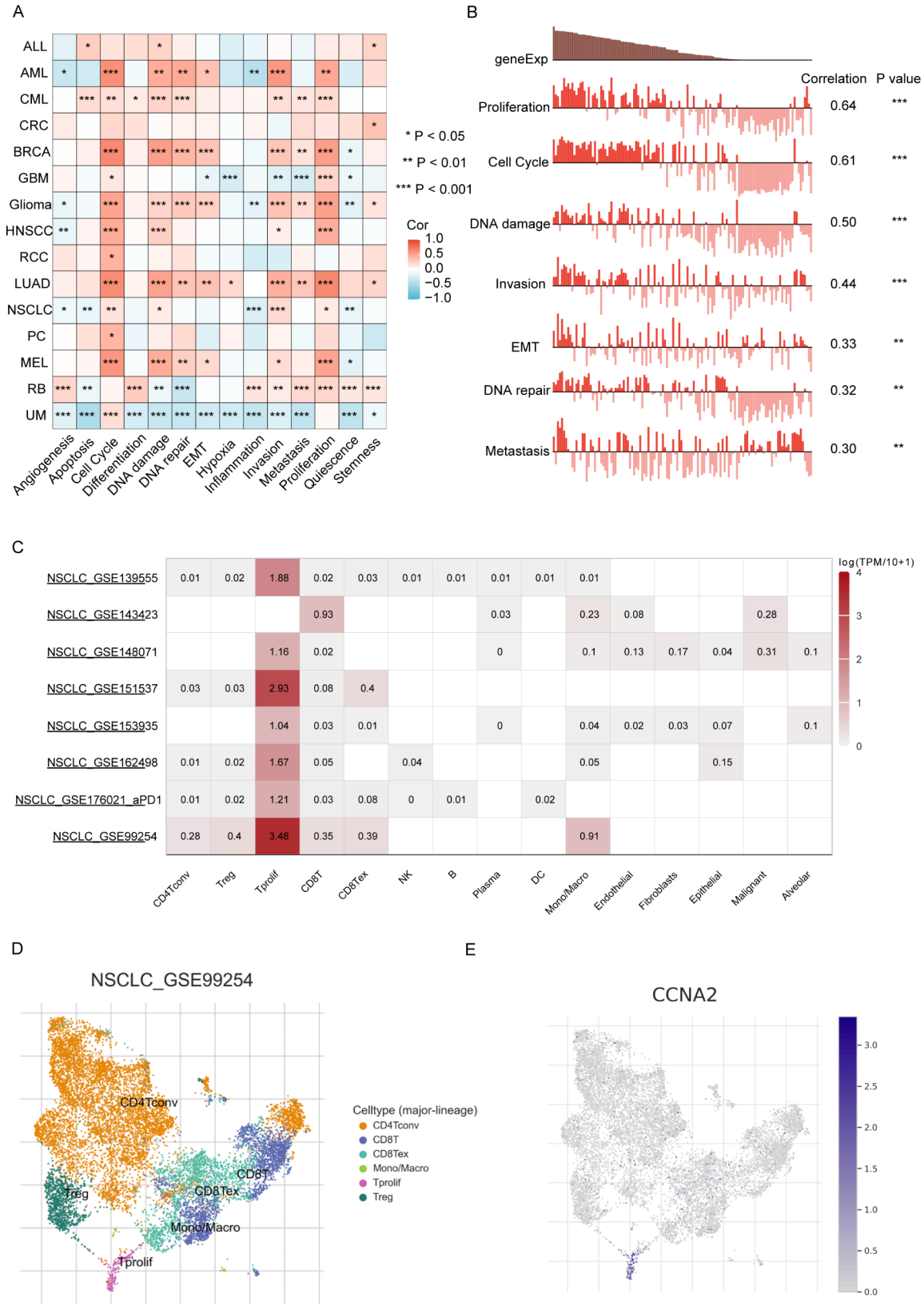

Fig. 7 CCNA2 expression at single-cell level in NSCLC. (**A**) The relationship between CCNA2 expression and different functional states in tumors was explored by CancerSEA. (**B**) Correlation analysis between functional status and CCNA2 expression in LUAD. (**C**) CCNA2 expression profiles at single-cell resolution of NSCLC from TISCH2. (**D**) The representative single-cell sequencing diagram illustrating CCNA2 predominantly expressed in Tprolif cells in NSCLC_GSE99254 dataset. **P* < 0.05, ***P* < 0.01, and ****P* < 0.001

(Fig. 7B). More precise single-cell sequencing results indicated that CCNA2 was mainly expressed highly in Tprolif cells in NSCLC_GSE139555, GSE148071, GSE151537, GSE153935, GSE162498, GSE176021_aPD1 and GSE99254 from TISCH 2 (Fig. 7C). Of note, in NSCLC_GSE99254, high expression level of CCNA2 was found predominantly occur in Tprolif cells, suggesting a potential role for CCNA2 in the TME in NSCLC (Fig. 7D-E).

Discussion

Lung cancer is among the most detrimental malignant neoplasms to human health and longevity, with NSCLC comprising the majority of its pathological subtypes. Despite considerable progress in the diagnostic and therapeutic approaches for NSCLC, the five-year survival rate continues to be dishearteningly low. Therefore, it is imperative to delve into the pathophysiology of NSCLC and to pinpoint novel therapeutic targets. Our study's findings indicate that CCNA2 may serve as a promising biomarker for the diagnosis, prognosis, and possibly the immunological treatment of NSCLC.

Through screening of the GEO database, we identified 10 hub genes (TTK, BUB1B, CCNA2, UBE2C, AURKB, MELK, CCNB2, KIF2C, CDCA8, NUSAP1) are potentially pivotal to the prognosis of NSCLC. Current research indicates that these core genes could serve as either oncogenes or promising biomarkers for tumorigenesis. According to research by Yang et al., TTK can be employed as a prognostic biomarker of endometrial cancer [24]. Prostate cancer progression and cell proliferation can be impeded by TTK down-regulation [25]. It has been reported that BUB1B is a type of spindle assembly checkpoint gene essential for the occurrence and growth of breast cancer cells [26]. BUB1B can accelerate the development of extrahepatic cholangiocarcinoma and hepatocellular carcinoma by activating the mTORC1 signaling pathway [27]. Liu et al. discovered that UBE2C was substantially expressed in endometrial cancer tissues. Up-regulation of UBE2C was linked to an advanced FIGO (International federation of gynecology and obstetrics) stage, recurrence, and worse OS. Endometrial cancer cell proliferation, migration, invasion, and EMT were all reduced by UBE2C knockdown [28]. A promising biomarker for the prognosis of patients with clear cell renal cell carcinoma (ccRCC) can be used since high expression of AURKB indicates an adverse prognosis in ccRCC patients [29]. MELK, a kinase implicated in oncogenesis, is associated with tumor mitosis and has been shown to accelerate the progression of endometrial cancer by activating the mTOR signaling pathway [30]. Tian et al. reported that BUB1B can control the transcription of MELK and accelerate the evolution of prostate cancer [31]. CCNB2 is a biomarker for an adverse prognosis in NSCLC patients. The proliferation, invasion and metastasis of NSCLC can be impacted through the regulation of CCNB2 by miR-335-5p [32]. Shi et al. reported that KIF2C is overexpressed in hepatocellular carcinoma, whose up-regulation is associated with unfavorable prognosis. KIF2C can mediate Wnt/b-catenin and mTORC1 signaling to accelerate disease progression [33]. In bladder cancer, CDCA8 is substantially expressed and associated with unfavorable clinicopathological characteristics of bladder cancer patients. Bladder cancer cells can be made more susceptible to apoptosis by CDCA8 knockdown [34, 35]. NUSAP1, often referred to as nucleolar and spindle-associated protein 1, controls the growth, metastasis and treatment resistance of tumor cells. Research shows that myocyte enhancer 2D (MEF2D) directly targets the NUSAP1 promoter and speeds up the development of NSCLC by triggering Wnt/b-catenin signal transduction [36]. Therefore, the current scientific literature suggests that these pivotal genes may function as oncogenes and also hold potential as biomarkers for the genesis and prognosis of tumors.

Previous investigations have established an association between CCNA2 and a spectrum of cancers, including its involvement in the pathogenesis of esophageal cancer, oral squamous cell carcinoma, and osteosarcoma. In the present study, it has been found that CCNA2 is overexpressed in NSCLC tissues and substantially associated with advanced tumor stage and lymph node metastasis. Our findings revealed that the expression of CCNA2 mRNA was most pronounced in Stage II and N4 categories, suggesting that CCNA2 may hold greater accuracy and utility in the diagnosis of intermediate and advanced stages of NSCLC. Notably, among the top CCNA2-interacted proteins from STRING (data not shown), CDC6 has been identified as a prognostic marker for ccRCC and hepatocellular carcinoma [37, 38]. CDK2 is associated with the cell division cycle [39]. E2F1 has been associated with cancer cell invasion, metastasis, and poor prognosis [40]. Thus, it is evident that CCNA2 exerts its influence not only in the context of lung cancer but also across various cellular processes.

In recent years, a growing body of research has identified aberrant cell cycle progression as one of the fundamental processes underlying cancer development. The present enrichment analysis has indicated that CCNA2 may contribute to the pathogenesis of NSCLC through its involvement in the cellular carcinogenesis and cell cycle. CCNA2 is mostly located in the nucleus as a critical cell cycle-regulating molecule. Chen et al. discovered that Yin Yang-1 (YY1) directly regulates Roundabout 1 (Robo1) via the CCNA2/CDK2 axis, thereby preventing the occurrence and progression of pancreatic cancer (PC) [41]. Guo et al. discovered that miR-508-3p reduces CCNA2 proliferation by specifically targeting

the 3-untranslated region (UTR) of ovarian cancer [42]. Our study aligns with previous research indicating that CCNA2 is significantly overexpressed in LUAD and is associated with smoking. This overexpression is linked to the promotion of tumorigenesis by boosting AT2/AT2-like cell differentiation, as suggested by single-cell sequencing analyses [43]. Literature has reported that Tanshinone IIA inhibits the progression of LUAD by regulating the CCNA2-CDK2 complex and the AURKA/PLK1 pathway [44]. Studies have shown that CCNA2 promotes EMT in NSCLC, which is a key process in cancer metastasis. This finding is significant as it links CCNA2 to the aggressive behavior of lung cancer cells [45]. CCNA2 has been identified as a hub gene in various cancer types, including LUAD, LUSC, and others, indicating its essential role across multiple malignancies. This pan-cancer evidence for CCNA2 highlights its broad significance in oncology [46]. In addition, the elevated expression of CCNA2 is associated with a poor prognosis of NSCLC, which is consistent with our findings [47]. CCNA2 is highly expressed in tumor tissues and positively regulates tumor-killing immune cells within the tumor microenvironment, which helps to activate $CD8^+$ T cells, enabling them to exert their cytotoxic effects on cancer cells, thereby extending the survival time of patients with colon cancer [48]. CCNA2 can modulate the function of macrophages, with higher expression levels of M2-type macrophages in tumors that highly express CCNA2 [49].

The TME is the environment in which the tumor, invasive immune cells, and stromal cells thrive. Numerous studies have demonstrated the importance of immunocyte infiltration in both the development of tumors and immunotherapy. Thus, it is crucial to conduct deeper investigation into the connection between CCNA2 and tumor-associated immune cell infiltration. In addition, the Tprolif cells are highly proliferative cells and play an important role in the immune system. They are a kind of lymphocytes with immunomodulatory function, which can release a variety of immune regulatory factors, regulate the immune response of the body and participate in the maintenance of immune balance. The results of single cell sequencing analysis showed that CCNA2 was mainly enriched in Tprolif cells in NSCLC. Additionally, there is a positive correlation between the expression of CCNA2 and common immunological checkpoints in most tumors, indicating that CCNA2 may be a potential target for tumor immunotherapy.

To sum up, our study supports CCNA2 as a potential new biomarker for the diagnosis and prognosis of NSCLC. Nevertheless, despite the aforementioned findings, our research has certain limitations. Future studies should include more in vivo and in vitro experiments for a detailed analysis. The NSCLC sample size in this study is modest, and the collection period was relatively brief, which constrains the scope of our findings. To better evaluate the prognostic significance of CCNA2, a more extended timeframe is necessary. In subsequent research, we aim to expand our sample size and incorporate more comprehensive clinical data to bolster the persuasiveness of our experimental results. However, our findings have been corroborated by additional studies and verification efforts, potentially providing a novel perspective for NSCLC research.

Conclusion

In summary, our research has demonstrated that CCNA2 is significantly upregulated in NSCLC and exhibits a notable correlation with the clinicopathological characteristics of NSCLC patients. This finding suggests that CCNA2 has the potential to serve as a reliable biomarker, with implications for both the diagnosis and the prognosis of NSCLC. Additionally, our study has identified a close association between CCNA2 expression levels and the infiltration of immune cells within the tumor microenvironment. Given these insights, targeting CCNA2 may represent a promising therapeutic avenue for the clinical management of NSCLC in the future.

Supplementary Information

The online version contains supplementary material available at https://doi.org/10.1186/s12890-025-03490-7.

Supplementary Material 1

Supplementary Material 2: Fig. 1. GO/KEGG enrichment analysis of the DEGs in GSE 18,842, GSE101929 and GSE116959.

Supplementary Material 3: Fig. 2. The mRNA expression of the ten hub genes in NSCLC. (A) TTK (B) BUB1B (C) CCNA2 (D) UBE2C (E) AURKB (F) MELK (G) CCNB2 (H) KIF2C (I) CDCA8 (J) NUSAP1. *$P < 0.05$.

Supplementary Material 4: Fig. 3. The prognostic value of the ten hub genes in NSCLC patients. (A) TTK (B) BUB1B (C) CCNA2 (D) UBE2C (E) AURKB (F) MELK (G) CCNB2 (H) KIF2C (I) CDCA8 (J) NUSAP1.

Acknowledgements

AcknowledgementsWe would like to thank the public database (TCGA, GEO, GEPIA, UALCAN, HPA, Kaplan-Meier Plotter, STRING, CancerSEA and TISCH2) and everyone involved in this study.

Author contributions

CRediT authorship contribution statementLiming Zhang: Writing - original draft, Investigation, Software, Methodology, Visualization, Funding acquisition. Shaoqiang Wang: Writing - review & editing, Resources, Software, Funding acquisition, Supervision. Lina Wang: Conceptualization, Formal analysis, Data curation, Writing - review & editing, Validation, Funding acquisition, Project administration.

Funding

This work was supported by the Scientific Research Plan of Weifang Health Commission (WFWSJK-2024-028), and National Natural Science Foundation of China (81800182, 81802290). The funders had no role in study design, data collection and analysis, decision to publish, or preparation of the manuscript.

Data availability
All datasets are publicly available. The GEO database is available via the following link: https://www.ncbi.nlm.nih.gov/geo/. The DAVID websites available via https://david.ncifcrf.gov/. The STRING database is available via https://cn.string-db.org/. Gene Expression Profiling Interactive Analysis (GEPIA) is available via http://gepia.cancer-pku.cn/index.html. The Kaplan-Meier plotter is publicly available via https://kmplot.com/analysis. TCGA dataset is available via the following link: https://portal.gdc.cancer.gov/. The Human Protein Atlas (HPA) database is available in the public domain via the following link: www.proteinatlas.org. CancerSEA is available via the following link: http://biocc.hrbmu.edu.cn/CancerSEA/. TISCH2 is available via the following link: http://tisch.comp-genomics.org.

Declarations

Ethics approval and consent to participate
All research involving human data in this study was conducted in accordance with the principles of the Declaration of Helsinki. The study was approved by the Ethics Committee of the Affiliated Hospital of Jining Medical University (Approval number 2021-11-C009). All participants provided informed consent prior to their involvement in the study.

Consent for publication
Not applicable.

Competing interests
The authors declare no competing interests.

Received: 7 November 2024 / Accepted: 8 January 2025
Published online: 11 January 2025

References

1. Bray F, Laversanne M, Sung H, Ferlay J, Siegel RL, Soerjomataram I, Jemal A. Global cancer statistics 2022: GLOBOCAN estimates of incidence and mortality worldwide for 36 cancers in 185 countries. CA Cancer J Clin 2024.
2. Arbour KC, Riely GJ. Systemic therapy for locally Advanced and Metastatic Non-small Cell Lung Cancer: a review. JAMA. 2019;322(8):764–74.
3. Silva Cascales H, Burdova K, Middleton A, Kuzin V, Müllers E, Stoy H, Baranello L, Macurek L, Lindqvist A. Cyclin A2 localises in the cytoplasm at the S/G2 transition to activate PLK1. Life Sci Alliance 2021, 4(3).
4. Deng H, Cheng Y, Guo Z, Zhang F, Lu X, Feng L, Wang X, Xu Z. Overexpression of CyclinA2 ameliorates hypoxia-impaired proliferation of cardiomyocytes. Exp Ther Med. 2014;8(5):1513–7.
5. Zhong C, Han Y, Ma J, Zhang X, Sun M, Wang Y, Chen J, Mi W, Xu X, Qiu J. Viral-mediated expression of c-Myc and cyclin A2 induces cochlear progenitor cell proliferation. Neurosci Lett. 2015;591:93–8.
6. Cheung CT, Bendris N, Paul C, Hamieh A, Anouar Y, Hahne M, Blanchard JM, Lemmers B. Cyclin A2 modulates EMT via β-catenin and phospholipase C pathways. Carcinogenesis. 2015;36(8):914–24.
7. Li T, Liu D, Li C, Ru L, Wang X. Silencing of LncRNA AFAP1-AS1 inhibits cell proliferation in oral squamous Cancer by suppressing CCNA2. Cancer Manag Res. 2021;13:7897–908.
8. Lu Y, Su F, Yang H, Xiao Y, Zhang X, Su H, Zhang T, Bai Y, Ling X. E2F1 transcriptionally regulates CCNA2 expression to promote triple negative breast cancer tumorigenicity. Cancer Biomark. 2022;33(1):57–70.
9. Wang H, Liu Z, Wu P, Wang H, Ren W. NUSAP1 accelerates Osteosarcoma Cell Proliferation and Cell Cycle Progression via Upregulating CDC20 and cyclin A2. Onco Targets Ther. 2021;14:3443–54.
10. Di Y, Zhang H, Zhang B, Li T, Li D. CCNA2 and KIF23 are molecular targets for the prognosis of adenoid cystic carcinoma. Aging 2024, 16.
11. Ma Q. MiR-219-5p suppresses cell proliferation and cell cycle progression in esophageal squamous cell carcinoma by targeting CCNA2. Cell Mol Biol Lett. 2019;24:4.
12. Davis S, Meltzer PS. GEOquery: a bridge between the Gene expression Omnibus (GEO) and BioConductor. Bioinformatics. 2007;23(14):1846–7.
13. Huang da W, Sherman BT, Lempicki RA. Systematic and integrative analysis of large gene lists using DAVID bioinformatics resources. Nat Protoc. 2009;4(1):44–57.
14. Sherman BT, Hao M, Qiu J, Jiao X, Baseler MW, Lane HC, Imamichi T, Chang W. DAVID: a web server for functional enrichment analysis and functional annotation of gene lists (2021 update). Nucleic Acids Res. 2022;50(W1):W216–21.
15. Szklarczyk D, Morris JH, Cook H, Kuhn M, Wyder S, Simonovic M, Santos A, Doncheva NT, Roth A, Bork P, et al. The STRING database in 2017: quality-controlled protein-protein association networks, made broadly accessible. Nucleic Acids Res. 2017;45(D1):D362–8.
16. Lopes CT, Franz M, Kazi F, Donaldson SL, Morris Q, Bader GD. Cytoscape web: an interactive web-based network browser. Bioinformatics. 2010;26(18):2347–8.
17. Tang Z, Li C, Kang B, Gao G, Li C, Zhang Z. GEPIA: a web server for cancer and normal gene expression profiling and interactive analyses. Nucleic Acids Res. 2017;45(W1):W98–102.
18. Győrffy B. Transcriptome-level discovery of survival-associated biomarkers and therapy targets in non-small-cell lung cancer. Br J Pharmacol. 2024;181(3):362–74.
19. Navani S. Manual evaluation of tissue microarrays in a high-throughput research project: the contribution of Indian surgical pathology to the human protein atlas (HPA) project. Proteomics. 2016;16(8):1266–70.
20. Chandrashekar DS, Karthikeyan SK, Korla PK, Patel H, Shovon AR, Athar M, Netto GJ, Qin ZS, Kumar S, Manne U, et al. UALCAN: an update to the integrated cancer data analysis platform. Neoplasia. 2022;25:18–27.
21. Chandrashekar DS, Bashel B, Balasubramanya SAH, Creighton CJ, Ponce-Rodriguez I, Chakravarthi B, Varambally S. UALCAN: a portal for facilitating Tumor Subgroup Gene expression and survival analyses. Neoplasia. 2017;19(8):649–58.
22. Yuan H, Yan M, Zhang G, Liu W, Deng C, Liao G, Xu L, Luo T, Yan H, Long Z, et al. CancerSEA: a cancer single-cell state atlas. Nucleic Acids Res. 2019;47(D1):D900–8.
23. Han Y, Wang Y, Dong X, Sun D, Liu Z, Yue J, Wang H, Li T, Wang C. TISCH2: expanded datasets and new tools for single-cell transcriptome analyses of the tumor microenvironment. Nucleic Acids Res. 2023;51(D1):D1425–31.
24. Yang Q, Yu B, Sun J. TTK, CDC25A, and ESPL1 as Prognostic Biomarkers for Endometrial Cancer. Biomed Res Int 2020, 2020:4625123.
25. Chen S, Wang J, Wang L, Peng H, Xiao L, Li C, Lin D, Yang K. Silencing TTK expression inhibits the proliferation and progression of prostate cancer. Exp Cell Res. 2019;385(1):111669.
26. Koyuncu D, Sharma U, Goka ET, Lippman ME. Spindle assembly checkpoint gene BUB1B is essential in breast cancer cell survival. Breast Cancer Res Treat. 2021;185(2):331–41.
27. Qiu J, Zhang S, Wang P, Wang H, Sha B, Peng H, Ju Z, Rao J, Lu L. BUB1B promotes hepatocellular carcinoma progression via activation of the mTORC1 signaling pathway. Cancer Med. 2020;9(21):8159–72.
28. Liu Y, Zhao R, Chi S, Zhang W, Xiao C, Zhou X, Zhao Y, Wang H. UBE2C is upregulated by Estrogen and promotes epithelial-mesenchymal transition via p53 in Endometrial Cancer. Mol Cancer Res. 2020;18(2):204–15.
29. Wan B, Huang Y, Liu B, Lu L, Lv C. AURKB: a promising biomarker in clear cell renal cell carcinoma. PeerJ. 2019;7:e7718.
30. Xu Q, Ge Q, Zhou Y, Yang B, Yang Q, Jiang S, Jiang R, Ai Z, Zhang Z, Teng Y. MELK promotes endometrial carcinoma progression via activating mTOR signaling pathway. EBioMedicine. 2020;51:102609.
31. Tian JH, Mu LJ, Wang MY, Zeng J, Long QZ, Guan B, Wang W, Jiang YM, Bai XJ, Du YF. BUB1B promotes proliferation of prostate Cancer via Transcriptional Regulation of MELK. Anticancer Agents Med Chem. 2020;20(9):1140–6.
32. Qian X, Song X, He Y, Yang Z, Sun T, Wang J, Zhu G, Xing W, You C. CCNB2 overexpression is a poor prognostic biomarker in Chinese NSCLC patients. Biomed Pharmacother. 2015;74:222–7.
33. Wei S, Dai M, Zhang C, Teng K, Wang F, Li H, Sun W, Feng Z, Kang T, Guan X, et al. KIF2C: a novel link between Wnt/β-catenin and mTORC1 signaling in the pathogenesis of hepatocellular carcinoma. Protein Cell. 2021;12(10):788–809.
34. Bi Y, Chen S, Jiang J, Yao J, Wang G, Zhou Q, Li S. CDCA8 expression and its clinical relevance in patients with bladder cancer. Med (Baltim). 2018;97(34):e11899.
35. Gao X, Wen X, He H, Zheng L, Yang Y, Yang J, Liu H, Zhou X, Yang C, Chen Y, et al. Knockdown of CDCA8 inhibits the proliferation and enhances the apoptosis of bladder cancer cells. PeerJ. 2020;8:e9078.
36. Ling B, Wei P, Xiao J, Cen B, Wei H, Feng X, Ye G, Li S, Zhang Z, Liang W, et al. Nucleolar and spindle–associated protein 1 promotes non–small cell lung cancer progression and serves as an effector of myocyte enhancer factor 2D. Oncol Rep. 2021;45(3):1044–58.

37. Temiz MZ. Commentary: increased CDC6 expression associates with poor prognosis in patients with Clear Cell Renal Cell Carcinoma. Front Oncol. 2021;11:730782.
38. Kong DG, Yao FZ. CDC6 is a possible biomarker for hepatocellular carcinoma. Int J Clin Exp Pathol. 2021;14(7):811–8.
39. Wang J, Liu X, Chu H, Chen J. Cell division cycle associated 2 (CDCA2) upregulation promotes the progression of hepatocellular carcinoma in a p53-dependant manner. PeerJ. 2022;10:e13535.
40. Yang J, Ying Y, Zeng X, Liu J, Xie Y, Deng Z, Hu Z, Li Z. Transcription factor E2F1 exacerbates papillary thyroid carcinoma cell growth and invasion via upregulation of LINC00152. Anal Cell Pathol (Amst) 2022, 2022:7081611.
41. Chen Q, Shen P, Ge WL, Yang TY, Wang WJ, Meng LD, Huang XM, Zhang YH, Cao SJ, Miao Y, et al. Roundabout homolog 1 inhibits proliferation via the YY1-ROBO1-CCNA2-CDK2 axis in human pancreatic cancer. Oncogene. 2021;40(15):2772–84.
42. Guo F, Zhang K, Li M, Cui L, Liu G, Yan Y, Tian W, Teng F, Zhang Y, Gao C, et al. miR–508–3p suppresses the development of ovarian carcinoma by targeting CCNA2 and MMP7. Int J Oncol. 2020;57(1):264–76.
43. He Q, Qu M, Xu C, Wu L, Xu Y, Su J, Bao H, Shen T, He Y, Cai J, et al. Smoking-induced CCNA2 expression promotes lung adenocarcinoma tumorigenesis by boosting AT2/AT2-like cell differentiation. Cancer Lett. 2024;592:216922.
44. Li Z, Zhang Y, Zhou Y, Wang F, Yin C, Ding L, Zhang S. Tanshinone IIA suppresses the progression of lung adenocarcinoma through regulating CCNA2-CDK2 complex and AURKA/PLK1 pathway. Sci Rep. 2021;11(1):23681.
45. Ruan JS, Zhou H, Yang L, Wang L, Jiang ZS, Wang SM. CCNA2 facilitates epithelial-to-mesenchymal transition via the integrin αvβ3 signaling in NSCLC. Int J Clin Exp Pathol. 2017;10(8):8324–33.
46. Chen S, Zhao Z, Wang X, Zhang Q, Lyu L, Tang B. The predictive competing endogenous RNA Regulatory Networks and potential prognostic and immunological roles of cyclin A2 in Pan-cancer Analysis. Front Mol Biosci. 2022;9:809509.
47. Gong K, Zhou H, Liu H, Xie T, Luo Y, Guo H, Chen J, Tan Z, Yang Y, Xie L. Identification and integrate analysis of key biomarkers for diagnosis and prognosis of Non-small Cell Lung Cancer based on Bioinformatics Analysis. Technol Cancer Res Treat. 2021;20:15330338211060202.
48. Li J, Zhou L, Liu Y, Yang L, Jiang D, Li K, Xie S, Wang X, Wang S. Comprehensive Analysis of Cyclin Family Gene expression in Colon cancer. Front Oncol. 2021;11:674394.
49. Xu Y, Wu G, Li J, Li J, Ruan N, Ma L, Han X, Wei Y, Li L, Zhang H et al. Screening and Identification of Key Biomarkers for Bladder Cancer: A Study Based on TCGA and GEO Data. *Biomed Res Int* 2020, 2020:8283401.

Publisher's note